

# Evaluation of corrosion level of naturally corroded bars using different cleaning methods, computed tomography, and 3D optical scanning

Ignasi Fernandez  · Karin Lundgren · Kamyab Zandi

Received: 8 August 2017 / Accepted: 6 June 2018 / Published online: 14 June 2018  
© The Author(s) 2018

**Abstract** Reliable methods are necessary to assess the corrosion level to establish links between structural performance and reinforcement corrosion in concrete structures. Hence, in this study, a set of naturally corroded bars were subjected to metallic brushing, acid immersion, and sandblasting for rust removal. Additionally, 3D optical, CT scanning, and weight loss measurements were used to evaluate the levels of corrosion. The results indicate that sandblasting is an optimal cleaning method. Weight loss measurements are sufficient when detailed information about corrosion is not required, and 3D scanning is preferred if information on corrosion variation along the bar is needed.

**Keywords** Corrosion level measurement · Cleaning methods · 3D optical scanning · Computed tomography scanning · Sandblasting · Acid cleaning

## 1 Introduction

Corrosion of reinforced steel bars continues to be one of the most frequent and significant type of damage

that occurs in existing impaired reinforced concrete structures. Chloride ion ( $\text{Cl}^-$ ) and carbon dioxide ( $\text{CO}_2$ ) penetration from the structure's surrounding environment leads to the destabilization of passivity conditions provided by the surrounding concrete to the steel bar. This destroys the steel protective layer, termed as the passive layer, and subsequently initiates corrosion of the steel. Hence, volumetric expansion of corrosion products and cross-section reduction of the steel bar leads to damages in the structure. Rust expansion inside concrete generates significant internal pressure that induce splitting stresses in the concrete along the corroded reinforcement and harm the surrounding concrete. Splitting stresses are not well tolerated by concrete and result in cracking and eventually spalling of the concrete cover. The corrosion rate may increase when the reinforcement becomes more exposed, thus facilitating the deterioration processes.

Corrosion of reinforcement in concrete is examined widely by several previous studies. For example, several previous studies [1–4] addressed the structural effects of corrosion. Various studies investigated local aspects that addressed the effects of corrosion on bond behaviour [5–7], change in mechanical properties [8–11], and other corrosion related phenomena [12–15]. However, most existing studies were conducted under accelerated corrosion conditions. There is a paucity of research examining natural corrosion circumstances due to various difficulties [16–19].

---

I. Fernandez (✉) · K. Lundgren · K. Zandi  
Division of Structural Engineering, Department of Civil and Environmental Engineering, Chalmers University of Technology, 412 96 Göteborg, Sweden  
e-mail: ignasi.fernandez@chalmers.se

Therefore, there is a growing demand to continue experimenting with naturally corroded specimens to further validate, and even extend existing knowledge. However, irrespective of the origin of corrosion, all the fore-mentioned studies are based on the measurement of the actual corrosion level with respect to the affected steel reinforcement. Thus, it is extremely important to obtain consistent methods to assess the corrosion of the steel bar and to examine its detailed impact on the steel surface. The methods should allow acquisition of precise information detailing pit characteristics and a faster and detailed measurement of the level of corrosion for a specific bar length. Simultaneously, the availability of reliable and more detailed information about the corrosion distribution will allow the establishment of increasingly trustworthy links between these measurements with respect to the structural response. Typically, existing studies have based the assessment of the corrosion level on the ASTM G1—Standard Practice for Preparing, Cleaning, and Evaluating Corrosion Test Specimens [20]. A few studies attempted to incorporate new techniques and technologies from other fields that theoretically provided a better description of the corrosion level along a steel bar [9, 21–26]. Nevertheless, all the aforementioned techniques are yet strongly dependent on the cleaning methods performed on the steel bars. A recent study by Tahershamsi et al. [27] pointed out significant discrepancies between obtained results using three-dimensional optical measurement (3D scanning) and weight loss measurement following metallic brush cleaning of naturally corroded steel bars. There is a paucity of similar studies that relate and compare different cleaning methods and corrosion level measurement techniques. An exception is the study conducted by Tang et al. [24] that presented a direct comparison between gravimetric and 3D scanning to assess the level of corrosion; the results indicated a very reasonable agreement; artificially corroded bars and sandblasting were used as cleaning methods.

Hence, the aim of the present study includes evaluating the scope and applicability of common cleaning methods used in existing studies as well as different measurement techniques to evaluate the corrosion level of naturally corroded bars. Consequently, a set of corroded steel bars extracted from a real bridge that is more than 30 years old was cleaned, and their levels of corrosion were assessed utilising

different techniques. The study involved examining and comparing the following three different cleaning methods to remove attached mortar and rust from the aforementioned specimens: (1) mechanical wire bristle brushing, (2) sandblasting, and (3) chemical cleaning. This was followed by applying and comparing the following three measurement techniques to evaluate the corrosion level: (1) weight loss, (2) 3D scanning, and (3) three-dimensional micro-computed tomography (CT scanning). The study presents the scope, applicability, and accuracy of each cleaning method along with its combination with the different measurement techniques. Furthermore, it details recommendations to obtain reliable levels of corrosion for the corroded steel bars.

## 2 Experimental programme

The specimens presented in the study are part of a larger experimental campaign conducted at Chalmers University of Technology in which specimens from edge beams of the Stallbacka Bridge in Sweden were used. The specimens were taken from the bridge when it was under repair following approximately 30 years of exposure to different natural deterioration phenomena such as corrosion induced by chlorides from de-icing salts. In an earlier study, beams were tested in four-point suspended bending tests to obtain anchorage failure [16, 17].

Table 1 presents an overview of all specimens included in this study on which different techniques were applied to measure the corrosion level. Each row indicates a specific enforced cleaning method including acid immersion, sandblasting, metallic brush, and no-cleaned before scanning and later cleaned using sandblasting. The various columns describe the number of specimens and the method used for the corrosion level evaluation for each group, specifically, weight loss, 3D scanning, and CT scanning.

### 2.1 Reinforcement steel bars

Tensile reinforcement steel bars were carefully extracted from a non-critical section of the beams. The beams contained two different 16-mm diameter bar types; both types of steel class Ks60 [28]. Each type involved different rib patterns, namely skewed



**Table 1** Overview of specimens, cleaning methods, and corrosion level evaluation methods

Cleaning method	Specimens (bars)	Corrosion level method		
		Weight loss	3D scanning	CT scanning
Acid	7	Yes	Yes	Yes
Sandblasting	7	Yes	Yes	Yes
No-cleaned <sup>a</sup>	7	Yes	No	Yes
Metallic brush <sup>b</sup>	17	Yes	Yes	No

<sup>a</sup>Specimens were first scanned and later cleaned by using sandblasting

<sup>b</sup>Specimens presented in a previous study [27]

and straight ribs. Only straight rib pattern bars were considered in this study.

### 2.1.1 Geometrical description of the bars

The steel bars were cut in lengths of 300 mm. This length was selected as a compromise between different requirements with respect to performed tasks. This included the maximum length that is allowed for subsequent CT scanning by using reasonable resolutions, the minimum length necessary for mechanical properties characterization by means of tensile tests, and a reasonable length for representativeness. Some studies have shown that pits are distributed stochastically along the bar length in [29]. Hence the choice of the specimen length should not have a relevant impact in the presented results; moreover, considering that the bars were extracted from the same structure, from zones that presented clear signs of deterioration, similar damage levels, and which had been exposed to similar aggressive environment, they are considered to be comparable.

The following bar specifications were measured from the uncorroded samples by using a Vernier Calliper with a resolution of 10  $\mu\text{m}$ , as shown in Fig. 1 and Table 2. The values given correspond to the measurement averages.

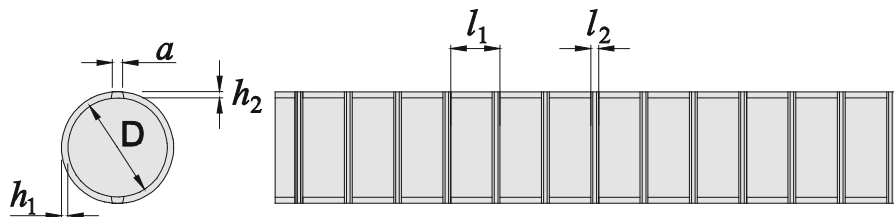


**Fig. 1** Geometry of ribbed reinforcement bars

### 2.1.2 Chemical composition

The chemical composition of the extracted steel was investigated by using scanning electron microscopy (SEM). The values presented in Table 3 correspond to the average values obtained for each component in different scanning points throughout the bar cross-section. Iron makes up to 100% of the steel composition.

### 2.2 Removal of corrosion products and assessment of the corrosion level

The extracted steel was cut into suitable parts with a length of 300 mm, and the bars were cleaned by using the following three most common methods found in literature: metallic bristle brushing, acid immersion, and sandblasting. Metallic bristle brushing is the most commonly used cleaning method [27, 30, 31]; this is mainly because it entails a low number of requirements for its use. Conversely, immersion in an acid solution is less common [7, 15, 32, 33]. As required by the specified standard [20], the weight loss was measured after several cleaning cycles. Additionally, some of the specimens were subject to two different scanning techniques, namely 3D and CT scanning; this allowed a description of the outer surface of the

**Table 2** Measured parameters and standard deviation to describe the geometry of the ribbed reinforcement bar (in mm)

Steel class	Nominal diameter	$D$	$\sigma$	$a$	$\sigma$	$h_1$	$\sigma$	$h_2$	$\sigma$	$l_1$	$\sigma$	$l_2$	$\sigma$	$\theta$ (°)
Ks60	Ø16	15.72	0.03	1.91	0.02	1.23	0.10	1.23	0.10	9.00	0.36	2.27	0.10	90

**Table 3** Chemical composition of the steel bars

	C	O	Si	Mn	Cr	Ni	Cu
Ks60	2.84	4.63	0.22	1.08	0.19	0.17	0.51

Each parameter is given in %

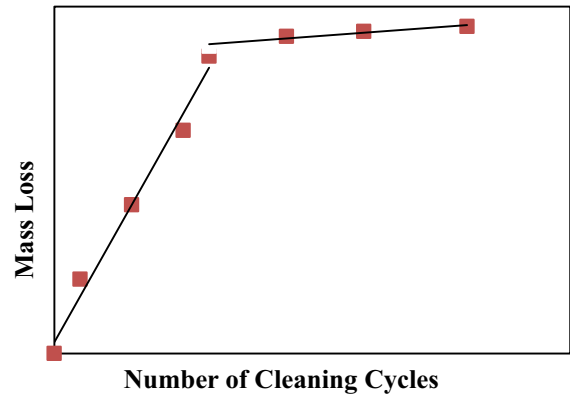
corroded bar and thereby permitted an evaluation of the corrosion level. Specifically, 3D and CT scanning techniques that are used widely in fields, such as industrial engineering or medicine, are not commonly used in civil engineering. Both techniques are relatively new, especially with respect to their application to deteriorated structures and their different structural elements. Thus, only a limited number of studies explored these methods and their applications [9, 22, 24, 30, 34, 35]. Furthermore, a group of specimens were scanned with the CT scanning technique prior to cleaning to assess whether the CT scanning technique was sufficiently effective to obtain a corrosion level without cleaning. This would involve time efficiency as well as a method to avoid possible induced inaccuracies of the cleaning methods.

### 2.2.1 Cleaning methods and weight loss measurement

The same procedure was followed for each of the cleaning methods used in this study. Reiterated cleaning cycles were applied to each specimen until the mass loss was lower than 0.2% of the previous measurement. Consequently, it was possible to clearly distinguish two different slopes as shown in Fig. 2. This necking point was not quantified in the ASTM recommendations [20] although this is used in the present study based on the harshness of the cleaning methods as detailed in subsequent sections.

A short description of each cleaning method performed on the steel bars is as follows:

- Mechanical brush was performed by utilising a rotational metallic wire bristle brush. It was attached to an engine plugged to an electricity

**Fig. 2** Standard recommendations for cleaning corroded steel bars [20]

supply, and the engine was in charge of continuously rotating the brush at the same speed. The recommendation [20] did not specify any cycle or exposition time, and thus each cycle was not systematically measured. Instead, each cycle was distinguished when perceptible changes on the surface due to the rust removing were observed after the bar was swept from end to end. According to this criterion, the necessary time for each cycle was approximately in the range of 10 min to 15 min based on the actual level of corrosion.

- Sandblasting was performed in an individual cabinet designed for the purpose. The sand was blasted at 5–7 bars of pressure. The sand employed for the rust removal corresponded to silica sand. Similarly, the recommendation followed for metallic brush [20] did not specify any cycle or exposition time. Hence, the same described criterion was used, and the bar was sandblasted from end to end until perceptible changes on the surface were observed. Accordingly, the necessary application time for each cycle was approximately less than 5 min.
- A wide range of chemical cleaning based methods are found in the ASTM recommendation [20]. The present study involved using the chemical cleaning method by repeated immersion of the bars in a

solution of hydrochloric acid and utropine (500 ml/l of solution hydrochloric acid, sp gr 1.19, 3.5 gr/l of solution hexamethylene tetramine and reagent water) in cycles that approximately lasted for 10 min. The selection choice was motivated by both safety rules and practical reasons since the other methods used carcinogenic products, high temperature environment, or very long exposition times.

The mass loss was measured after every cycle and the cycles were repeated until the aforementioned threshold was reached for each method.

Additionally, in order to obtain the scope of harshness of each cleaning method, uncorroded steel bars were cleaned, and the loss of sound steel was assessed with respect to each cleaning method. Acid and sandblasting cleaning yielded similar levels of sound steel removal that corresponded to approximately 0.2% of the initial weight. In contrast, metallic bristle brush had no significant impact in the non-corroded steel removing. Subsequently, the value of 0.2% weight loss between cycles was used in the present study as the threshold beyond which the bar was considered as fully cleaned. In addition to this threshold, it was also visually confirmed that the bars looked clean.

### 2.2.2 3D optical measurement technique

The 3D scanning of the corroded bars was performed by means of optical measurement. An industrial stereo device with two cameras of 5 Megapixels was used. The maximum accuracy provided by the cameras corresponded to 2  $\mu\text{m}$ , which allows the description of imperfections over the steel bar surface due to corrosion. A correction of the measurement inaccuracies, such as polygon spikes removing and mesh holes closing, and data treatment was performed using the post processing software Geomagic<sup>TM</sup> Wrap 2014 [36].

The outcome of the optical measurement corresponded to a very fine mesh of triangular surface polygons connected by nodes, see Fig. 3. The average size of the element corresponded to 0.014  $\text{mm}^2$  with a side length of approximately 0.15 mm. The number of triangular elements in each scanning was between 2,000,000 elements and 3,000,000 elements depending on the corrosion level. A global coordinate system,

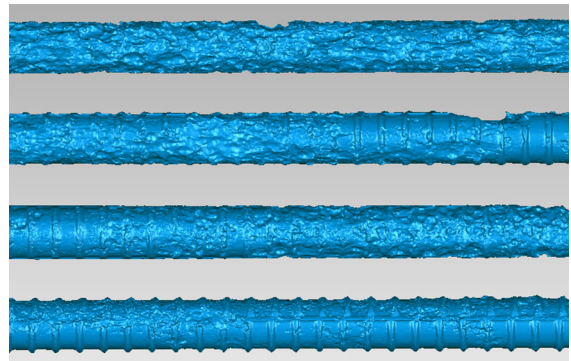


**Fig. 3** 3D surface generated from the 3D scanning

( $X, Y, Z$ ), was established and referenced to the end of the bar. The high resolution of the surface mesh allowed for a sufficiently detailed description of the geometry of the bar to obtain information on features including pit depth and length, pit distribution, and loss of cross-sectional area along the bar length.

### 2.2.3 Micro-computed tomography technique

Sound steel was determined using three-dimensional micro-computed tomography (CT scanning), which is used widely in image diagnostic medicine and is a promising technology that is also applicable to other fields such as civil engineering. Previous studies [22, 37, 38] used this technology to assess the effect of corrosion in concrete and mortar phases although very few studies focused on obtaining a comprehensive surface of corroded reinforcing bars [39].

Corroded steel bars were placed in a Metrotom<sup>®</sup> machine that projected X-Ray beams. As the steel bars were constituted by two clearly different materials, i.e. sound steel and corrosion products, different specific amounts of the X-Ray beam were absorbed by each one. It is possible to obtain a 2D image of the object by collecting the remaining transmitted intensity through the machine detector. The required intensity of the X-Ray beam was adjusted based on the material density, i.e., it must be sufficiently strong to penetrate the full thicknesses of the different components. The process is repeated several times conveyed to the rotation of the object within specific angles, and subsequently post-processing of the obtained images is performed to build a full 3D interpretation of the body. A larger difference between the densities of the materials that conform the object increases the degree

of ease and clarity of the result. The actual resolution of the flatbed-detector corresponded to a frame of  $1024 \times 1024$  pixels or a voxel of  $174 \mu\text{m}$  for 3D-CT scanning. Accordingly, in order to increase the final resolution of the final surface mesh of the steel, two scans together covering the total volume were performed which allowed the maximum accuracy by the equipment used. Subsequently, the two steel outcome surfaces were digitally stitched to form a unique full volume that contained all the defining points. The technology possesses the potential to describe the outer surface of the corroded steel bar in detail without cleaning the corrosion products in advance as they present very dissimilar densities.

The same type of surface mesh as that described for the 3D scanning technique that was previously presented was obtained by means of the CT scanning.

#### 2.2.4 Evaluation of the level of corrosion using scanning techniques

A method that was developed in a previous study [27] was used to determine the corrosion level variation along a bar based on the scanning measurements:

- The resulting outer geometry based on the scanning output is postprocessed, cleaned and repaired.
- The coordinates of the nodes are transformed into a polar coordinate system, and a contour plot of the corrosion penetration along the bar surface is created from the new points, which allows to visually observe the corrosion pits along the bar surface
- The cross-sectional area at specific sections uniformly separated is obtained by integration of the coordinates.
- The cross-sectional area along the bar is calculated and plotted. The bar corresponded to a ribbed bar, and thus the cross-sectional area varies along the bar. The effect of the ribs is eliminated by a smoothing fit that used cubic splines; this results in another curve. The uncorroded zone/s of the bar is/are identified, and the average cross-sectional area is used as a reference.
- The normalized cross-sectional reduction is plotted by dividing the measured cross-sectional area with respect to the uncorroded area.
- Finally, the corrosion level variation in percentage is plotted along the bar.

A complete description of the detailed steps from the initial 3D polygonal mesh to the graph that shows the cross-section variation is provided in a previous study [27].

### 3 Results and discussion

#### 3.1 Cleaning methods

Figure 4a shows the average mass loss of all bars cleaned with each cleaning method. The same proposed methodology [20] was followed for each cleaning method with reiterated cleaning cycles until the mass loss was lower than 0.2% of the last measured weight. However, large differences were observed in the final measurements between the three selected options as shown in Fig. 4a. The sandblasted specimens exhibited the largest measured corrosion level, systematically both for all the specimens, and for the average level of corrosion in each group. This was followed by the acid cleaned specimens. Finally, the mechanically brushed specimens exhibited the smallest measured corrosion level. The methods were expected to result in similar levels of the average mass loss, since the bars were randomly obtained from the tested beams, from areas which had been exposed to similar aggressive environment and subjected to similar damage (all the specimens presented clear signs of deterioration). Thus, the fore-mentioned discrepancies indicate that the proposed recommendations did not provide information to a user with respect to the degree of cleanness of the bar at the end of the process, as opposed to whether the performed cleaning method reached its maximum cleaning capacity for a set of specific conditions including steel type, initial amount of mortar, and corrosion products attached or cleaning agent (such as chemical, or brush). This assertion is backed by Fig. 4b, in which the average number of cycles applied to each specimen to reach the necking point together with its standard deviation is shown. It was observed that the number of cycles remained constant regardless the final level of corrosion.

As shown in Fig. 4b, the number of cycles necessary to obtain a weight loss difference lower than 0.2% within cycles (which was defined by the authors as a reference value based on the degree of harshness of the cleaning methods) ranged between 4 cycles and 7



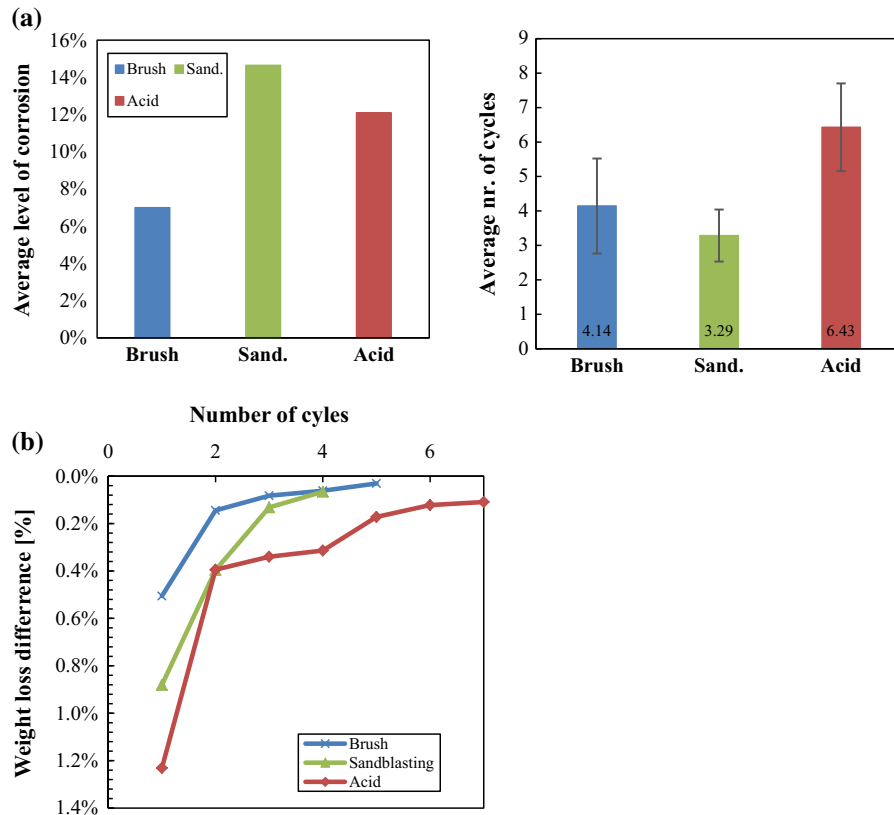


**Fig. 4** **a** Average mass loss for the different cleaning methods. **b** Examples of cleaning cycles for each cleaning method

cycles according to the method for representative specimens. Sandblasting reached its highest cleaning capacity in fewest number of cycles whereas acid immersion needed the highest number of cycles to reach the defined threshold. The cleaning speed of the metallic brush method ranged in between that of sandblasting and acid immersion on an average, although the scatter observed among the different bars increased in contrast to those observed in the other methods. This scatter could indicate higher dependence of the brush cleaning method on the actual corrosion level than the others.

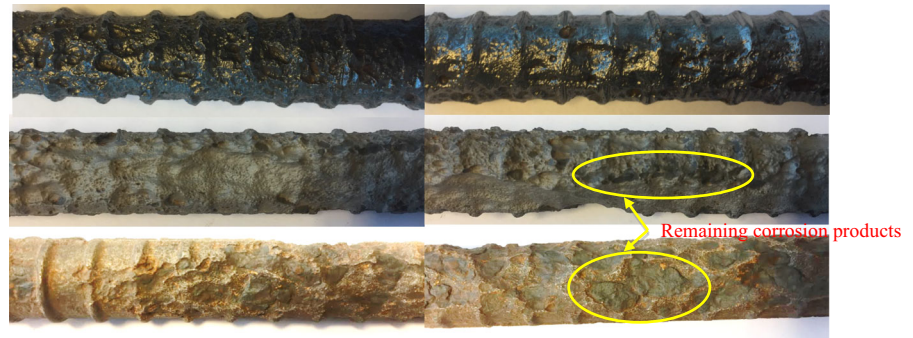
With respect to the cleaning time necessary to reach the proposed necking point, the results indicated that the maximum time to reach the proposed necking point corresponded to that of acid solution that required more than 70 min of immersion in addition to the drying and weighting time of the bars within cycles. However, acid cleaning allowed multiple bars to be simultaneously cleaned, i.e., several bars could be placed in the same recipient containing the acid

solution. Thus, the individual effective time with respect to the bar was considered lower and approximately corresponded to 15–20 min. The results revealed that sandblasting exhibited a very high speed and only required less than 20 min of application per single bar to reach the same cleaning capacity. Finally, metallic brush required the longest cleaning time per bar and the average corresponded to approximately 40 min based on the actual corrosion level.

However, direct conclusions to assess the actual accuracy of the method could not be extracted from the results after cleaning since the results only expressed a relative comparison with respect to the initial weight and did not provide any indication as to whether or not the bar was completely cleaned. Nevertheless, the maximum cleaning capacity was definitely reached for each method. Figure 5 shows a few bars after rust removal.

Important differences were observed in the final shape of the surface after cleaning. The finishes for the different methods corresponded to shiny and smooth

**Fig. 5** Cleaned bars. From top to bottom, the figure shows metallic brush, sandblasting, and acid immersion



for metallic brush, matt and granulated for sandblasting, and dark brown for acid cleaning. All the methods showed corrosion pits along the bar irrespective of the finish for each method. However, the depiction of pits was significantly more clear after sandblasting when compared to the other methods, as shown in Figs. 5 and 6. Subsequently, a more comprehensive impact of the corrosion on the bar surface was observed in which larger and deeper pits were found in the sandblasted bars as shown in Fig. 6. This was not obtained when the bars were extracted or when the bars were cleaned with the two other methods.

It should be noted that neither metallic brush nor acid immersion specimens portrayed any remaining corrosion products after the bars were cleaned. The shiny and smooth surfaces due to the metallic brush covered the remaining corrosion products attached to the bar. However, few pieces jumped off and the bars exhibited the aforementioned products when the bars were tested under a tensile load [27]. With respect to acid immersion, the surface after cleaning exhibited a homogeneous dark brown finish and did not allow the detection of the presence of remaining corrosion products. Clusters of corrosion products indicating the presence of a significant amount of rust attached to the

bar were only unveiled after a significant period of time elapsed as shown in Fig. 5. This was potentially due to the drying out of the acid solution and the occurrence of slight corrosion in the sound steel that changed the surface shade.

Conversely, sandblasted specimens always exhibited remaining rust clusters that were distributed along the bar during the cleaning cycles. Specifically, the mentioned clusters were also used as additional visual criteria to define the exposition time in each cycle. Nevertheless, there was a significantly lower presence of rust clusters at the necking point in the case for sandblasting when compared with acid cleaning as clearly shown in Fig. 5. The remaining corrosion products on the bar surface were a result of the compromise between the corrosion products and sound steel removed in each cycle, which must always be lower than the method harshness. Corrosion products, in addition to sound steel must be removed in the cycle in order to maintain the accuracy of the measured level of corrosion.

### 3.2 Assessment of the corrosion level, and a comparison between weight loss, CT, and 3D scanning

Table 4 lists the levels of corrosion obtained with the different techniques that are applied on each bar. Each value represents the average corrosion level along the specimen length, which corresponds to 300 mm. Hence, it was expected that presented values evaluated with the different techniques would be in agreement. However, major differences were observed and are discussed in the following section.

Figure 7 shows an overall description of the obtained results by means of depicting the average measurements. As shown in the figure, 3D scanning



**Fig. 6** Pits unveiled after sandblasting

**Table 4** Corrosion level results

Cleaning method	Specimen	Corrosion level (%)					
		Weight loss	Average	3D scanning	Average	CT scanning	Average
Acid	CA-1	12.1	8.78	10.3	6.96	9.9	6.66
	CA-2	13.3		10.8		10.7	
	CA-3	2.0		1.5		0.8	
	CA-4	4.5		2.8		2.6	
	CA-5	16.2		13.6		13.5	
	CA-6	4.4		3.2		2.8	
	CA-7	9.0		6.5		6.3	
Sandblasting	CA-8	17.1	11.05	16.5	10.64	15.0	9.29
	CA-9	11.1		10.6		9.3	
	CA-10	1.7		1.8		0.6	
	CA-11	13.9		13.4		12.1	
	CA-12	14.2		13.9		12.7	
	CA-13	11.9		11.3		9.5	
	CA-14	7.4		7.0		5.8	
Not-cleaned <sup>a</sup>	CA-15	12.2	8.7	–	–	3.9	2.085
	CA-16	8.4		–		0.8	
	CA-17	3.3		–		0.1	
	CA-18	7.4		–		2.1	
	CA-19	14.3		–		4.3	
	CA-20	9.5		–		2.2	
	CA-21	5.8		–		1.2	
Metallic brush <sup>b</sup>	CA-22	7.0	4.32	4.6	2.74	–	–
	CA-23	2.9		2.5		–	
	CA-24	1.6		0.8		–	
	CA-25	0.0		0.1		–	
	CA-26	6.7		3.7		–	
	CA-27	2.3		2.0		–	
	CA-28	9.0		4.3		–	
	CA-29	6.3		3.5		–	
	CA-30	2.3		1.9		–	
	CA-31	5.7		3.6		–	
	CA-32	7.8		6.2		–	
	CA-33	4.0		2.5		–	
	CA-34	2.6		1.4		–	
	CA-35	1.5		0.9		–	
	CA-36	1.4		0.7		–	
	CA-37	8.6		5.0		–	
	CA-38	3.7		2.8		–	

<sup>a</sup>Specimens that were scanned prior to cleaning and subsequently cleaned using sandblasting

<sup>b</sup>Specimens presented in a previous study [27]

resulted in higher values in all cases when compared to those obtained in CT scanning. However, the obtained values were consistently below the weight loss

measurement. Average 3D scanning and weight loss values described very good agreement with respect to sandblasting cleaning method, and the difference



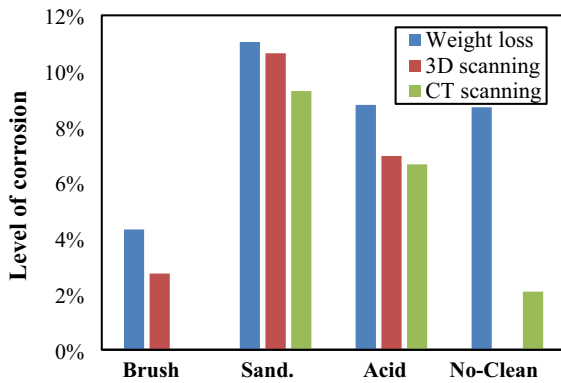
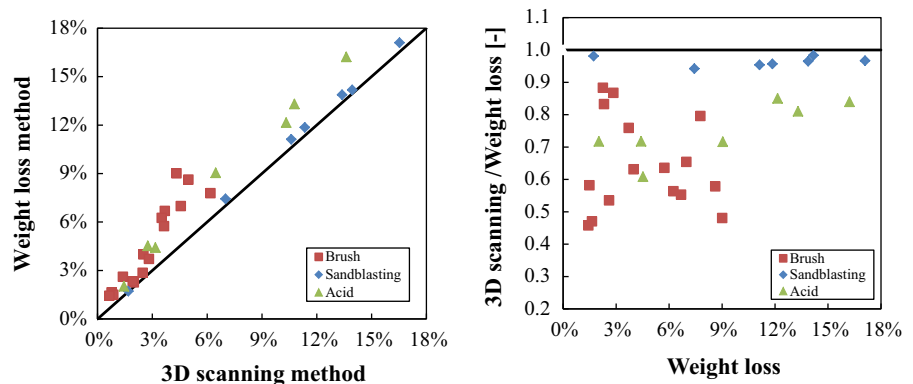


**Fig. 7** Average corrosion level for each presented method

between the average weight loss and that in CT scanning was higher for all the cleaning methods.

A direct comparison between single weight loss and 3D scanning corrosion levels for the three proposed cleaning methods is shown in Fig. 8a. As shown, gravimetric weight loss typically resulted in higher corrosion levels when compared with those from 3D scanning measurements irrespective of the utilised cleaning method. However, the results indicated better agreement between the weight loss and those of 3D scanning for the sandblasted bars wherein there was a minor difference between both methods. In contrast, both acid and metallic bristle brush exhibited higher deviations when compared to sandblasting. Metallic brush cleaning exhibited the maximum difference, and the obtained values followed a trend in which a higher corrosion level led to a higher discrepancy between both measurements. Additionally, the highest corrosion level measured using both weight loss and 3D scanning was observed for the sandblasted specimens, and this was followed by the acid and the metallic

**Fig. 8** Comparison of 3D scanning versus weight loss measurements for different cleaning methods



brush. This is potentially related to the efficiency of the cleaning method.

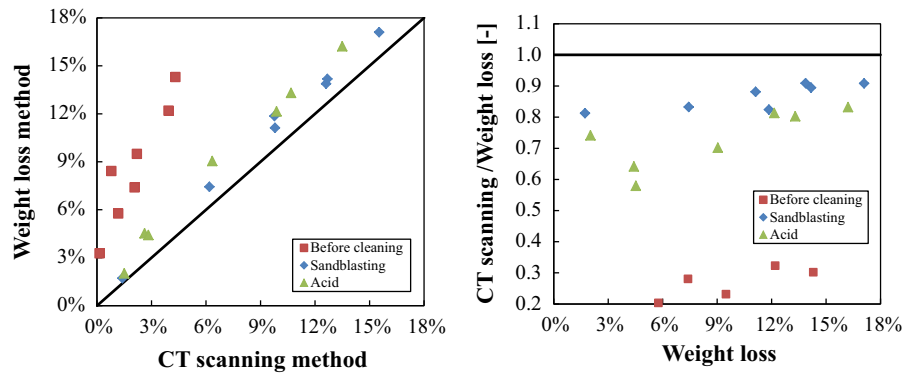
Generally, sandblasting cleaning yielded the best agreement irrespective of the actual corrosion level as shown in Fig. 8b by the ratio of 3D scanning to weight loss measurement. Acid cleaning exhibited a slightly better agreement when the corrosion level increased, and this indicated that the accuracy of the cleaning method was less relevant for increases in the corrosion level. Conversely, metallic brush cleaning displayed large scatter and a clear trend was not observed.

The same comparison for the CT scanning technique is presented in Fig. 9. The CT scanning measurements resulted in smaller corrosion levels when compared with the weight loss measurements. The same behaviour was observed for all the cleaning methods as well as for the bars scanned prior to cleaning. In a manner, similar to the 3D scanning results, the best agreement between CT scanning and weight measurements was exhibited by the sandblasted specimens while the bars scanned prior to cleaning showed the maximum disagreement.

On average, corrosion levels measured for the bars that were cleaned using sandblasting as preferred cleaning method were higher, followed by the bars cleaned by acid immersion and the uncleaned bars in terms of both weight loss and CT scanning measurements as shown in Fig. 8. This result along with the fact that the different bars were considered arbitrarily within the tested beams indicates that the accuracy of the rust removal was strongly dependent on the employed cleaning method.

The accuracy of both cleaning methods (acid and sandblasting) seemed to follow a trend that indicated that the accuracy of the cleaning method became less

**Fig. 9** Comparison of CT scanning versus weight loss measurement for different cleaning methods and prior to cleaning



relevant when higher corrosion levels were observed as shown in Fig. 9b, i.e. the more corroded the bar, the better the performance of the cleaning method. Nevertheless, the ratio of CT scanning to weight loss measurement did not correspond to values exceeding 0.9, which clearly showed a limitation of the accuracy of CT scanning. Furthermore, the corrosion level evaluation results of the uncleaned bars by using CT scanning technique revealed that the selected accuracy value was not sufficient to distinguish between the rust and steel, and consequently, it is necessary to carefully clean the bars prior to scanning.

#### 4 Conclusions

The following conclusions were obtained from the study:

- Major differences were observed in the results of the different cleaning methods:
  1. The results indicated that metallic brush was not sufficiently strong to remove all the corrosion products for naturally corroded bars. The fact that it was impossible to visually observe remaining corrosion products after cleaning, and the cleaned surface was shiny and smooth led to misleading interpretations. A comparison of the results with those obtained for the other methods, in conjunction with the observation that the pieces jumped off during tensile tests, strongly suggests that there were remaining corrosion products.
  2. Acid cleaning described reasonably good results. However, the method exhibited clear disadvantages such as requiring more cycles, being time

consuming, and possessing a lower removal capacity when compared to sandblasting. The surface finish also hid the remaining rust clusters, and this led to wrong conclusions with respect to the cleaning capacity since rust clusters were unveiled as time elapsed.

3. Sandblasting corresponded to the most efficient and reliable corrosion removal method. Larger and deeper pits were detected as in addition to a better definition of the corrosion impression on the bar surface. The obtained weight loss results agreed well with the different corrosion level attainment techniques.
  4. The harshness (i.e. unintended removal of sound steel) observed in acid immersion and sandblasting was similar and not significant. Brush cleaning presented almost no harshness.
- With respect to the different measurement methods:
    1. The 3D scanning displayed high reliability in the assessment of the corrosion level when the corroded bar was cleaned well although the 3D scanning results were very sensitive to the cleaning method used. The main advantage of this method is that it enables a detailed description of the pit geometry and the corrosion level variation relative to the studied length.
    2. The results revealed that CT scanning was not sufficiently accurate when applied to these types of large specimens. It is possible to use CT scanning with a higher accuracy if smaller specimens are used. However, the specimens are then considered as too small to be used for tensile tests, and a larger number of scans per bar are required.

The CT scanning technique appeared to be less sensitive to the cleaning method. Unfortunately, the technology used in this work did not possess the capacity to obtain reliable corrosion levels when the specimen was completely uncleaned.

3. The corrosion level attained by weight loss measurement corresponded to the most efficient and trustworthy measurement. The density of rust products is lower than that of the sound steel, and this strongly reduces the associated error of the cleaning methods. However, it was necessary to employ high efficiency cleaning methods, such as sandblasting and acid cleaning, to obtain reliable corrosion levels.

As a general conclusion, commonly used recommendations in previous studies [20] only warrant that the selected cleaning method has reached its maximum cleaning capacity, which does not unequivocally correspond to the actual corrosion level. Hence, the recommendations of the present study indicate that sandblasting should be used as a cleaning method for naturally corroded bars. Weight loss measurements are sufficient when detailed information on corrosion is not required while 3D scanning is recommended if information about the corrosion variation along the bar is needed.

**Funding** This work was undertaken at Chalmers University of Technology, Division of Structural Engineering, Concrete Structures. The authors would like to acknowledge the funding from the Swedish Transport Administration (Trafikverket).

#### Compliance with ethical standards

**Conflict of interest** The authors declare that they have no conflict of interest.

**Open Access** This article is distributed under the terms of the Creative Commons Attribution 4.0 International License (<http://creativecommons.org/licenses/by/4.0/>), which permits unrestricted use, distribution, and reproduction in any medium, provided you give appropriate credit to the original author(s) and the source, provide a link to the Creative Commons license, and indicate if changes were made.

#### References

1. Fernandez I, Herrador MF, Marí AR, Bairán JM (2016) Structural effects of steel reinforcement corrosion on statically indeterminate reinforced concrete members. *Mater Struct* 49(12):4959–4973
2. Law D, Du Y, Cairns J (2008) Structural performance of corrosion-damaged concrete beams. *Mag Concr Res* 60(5):359–370
3. Biondini F, Vergani M (2014) Deteriorating beam finite element for nonlinear analysis of concrete structures under corrosion. *Struct Infrastruct Eng* 11(4):519–532
4. Maalej M, Ahmed SFU, Paramasivam P (2003) Corrosion durability and structural response of functionally-graded concrete beams. *J Adv Concr Technol* 1(3):307–316
5. Lundgren K, Gylltoft K (2000) A model for the bond between concrete and reinforcement. *Mag Concr Res* 1:53–63
6. Casanova A, Jason L, Davenne L (2012) Bond slip model for the simulation of reinforced concrete structures. *Eng Struct* 39:66–78
7. Fernandez I, Etxeberria M, Marí AR (2016) Ultimate bond strength assessment of uncorroded and corroded reinforced recycled aggregate concretes. *Constr Build Mater* 111:543–555
8. Fernandez I, Bairán JM, Marí AR (2015) Corrosion effects on the mechanical properties of reinforcing steel bars. Fatigue and  $\sigma$ - $\epsilon$  behavior. *Constr Build Mater* 101:772–783
9. Ou Y-C, Susanto YTT, Roh H (2016) Tensile behavior of naturally and artificially corroded steel bars. *Constr Build Mater* 103:93–104
10. Lundgren K, Gylltoft K (2000) A model for the bond between concrete and reinforcement. *Mag Concr Res* 52(1):53–63
11. Apostolopoulos CA, Papadopoulos MP, Pantelakis SG (2006) Tensile behavior of corroded reinforcing steel bars BSt 500s. *Constr Build Mater* 20(9):782–789
12. Michel A, Solgaard AOS, Pease BJ, Geiker MR, Stang H, Olesen JF (2013) Experimental investigation of the relation between damage at the concrete-steel interface and initiation of reinforcement corrosion in plain and fibre reinforced concrete. *Corros Sci* 77:308–321
13. Michel A, Otieno M, Stang H, Geiker MR (2016) Propagation of steel corrosion in concrete: experimental and numerical investigations. *Cem Concr Compos* 70:171–182
14. Malumbela G, Alexander M, Moyo P (2010) Variation of steel loss and its effect on the ultimate flexural capacity of RC beams corroded and repaired under load. *Constr Build Mater* 24(6):1051–1059
15. Berrocal CG, Fernandez I, Lundgren K, Löfgren I (2017) Corrosion-induced cracking and bond behaviour of corroded reinforcement bars in SFRC. *Compos Part B Eng* 113:123–137
16. Tahershamsi M, Zandi K, Lundgren K, Plos M (2014) Anchorage of naturally corroded bars in reinforced concrete structures. *Mag Concr Res* 66(14):729–744
17. Lundgren K, Tahershamsi M, Zandi K, Plos M (2015) Tests on anchorage of naturally corroded reinforcement in concrete. *Mater Struct* 48(7):2009–2022
18. Zhu W, François R (2014) Experimental investigation of the relationships between residual cross-section shapes and the ductility of corroded bars. *Constr Build Mater* 69:335–345
19. Dang VH, François R (2013) Influence of long-term corrosion in chloride environment on mechanical behaviour of RC beam. *Eng Struct* 48:558–568
20. ASTM G1 (2011) Standard practice for preparing, cleaning, and evaluating corrosion test



21. Apostolopoulos CA, Demis S, Papadakis VG (2013) Chloride-induced corrosion of steel reinforcement—mechanical performance and pit depth analysis. *Constr Build Mater* 38:139–146
22. Fernandez I, Bairán JM, Marí AR (2016) 3D FEM model development from 3D optical measurement technique applied to corroded steel bars. *Constr Build Mater* 124:519–532
23. Mancini G, Tondolo F, Iuliano L, Minetola P (2014) Local reinforcing bar damage in r.c. members due to accelerated corrosion and loading. *Constr Build Mater* 69:116–123
24. Tang F, Lin Z, Chen G, Yi W (2014) Three-dimensional corrosion pit measurement and statistical mechanical degradation analysis of deformed steel bars subjected to accelerated corrosion. *Constr Build Mater* 70:104–117
25. Wang X, Zhang W, Gu X, Dai H (2013) Determination of residual cross-sectional areas of corroded bars in reinforced concrete structures using easy-to-measure variables. *Constr Build Mater* 38:846–853
26. Kashani MM, Crewe AJ, Alexander NA (2013) Use of a 3D optical measurement technique for stochastic corrosion pattern analysis of reinforcing bars subjected to accelerated corrosion. *Corros Sci* 73:208–221
27. Tahershamsi Mohammad, Fernandez Ignasi, Lundgren Karin, Zandi Kamyab (2016) Investigating correlations between crack width, corrosion level and anchorage capacity. *Struct Infrastruct Eng* 13(10):1294–1307. <https://doi.org/10.1080/15732479.2016.1263673>
28. Institudes SS (1971) Armeringsstång. Kamstång Ks 60 och Ks 60S (STD-1250), pp 1–4
29. Zhu W, François R, Poon CS, Dai J-G (2017) Influences of corrosion degree and corrosion morphology on the ductility of steel reinforcement. *Constr Build Mater* 148:297–306
30. Apostolopoulos CA, Demis S, Papadakis VG (2013) Chloride-induced corrosion of steel reinforcement—mechanical performance and pit depth analysis. *Constr Build Mater* 38:139–146
31. Du Y, Cullen M, Li C (2013) Structural performance of RC beams under simultaneous loading and reinforcement corrosion. *Constr Build Mater* 38:472–481
32. Zhang R, Castel A, François R (2009) The corrosion pattern of reinforcement and its influence on serviceability of reinforced concrete members in chloride environment. *Cem Concr Res* 39(11):1077–1086
33. Moreno Fernández E, Cobo Escamilla A, Fernández Cánovas M (2007) Ductility of reinforcing steel with different degrees of corrosion and the ‘equivalent steel’ criterion. *Mater Constr* 57:5–18
34. Mancini G, Tondolo F, Iuliano L, Minetola P (2014) Local reinforcing bar damage in r.c. members due to accelerated corrosion and loading. *Constr Build Mater* 69:116–123
35. Wang X, Zhang W, Gu X, Dai H (2013) Determination of residual cross-sectional areas of corroded bars in reinforced concrete structures using easy-to-measure variables. *Constr Build Mater* 38:846–853
36. 3D Systems, “Geomagic Wrap 2014”. <http://www.geomagic.com/en/>
37. Beck M, Goebbels J, Burkert A (2007) Application of X-ray tomography for the verification of corrosion processes in chloride contaminated mortar. *Mater Corros* 58(3):207–210
38. Šavija B, Luković M, Hosseini SAS, Pacheco J, Schlangen E (2015) Corrosion induced cover cracking studied by X-ray computed tomography, nanoindentation, and energy dispersive X-ray spectrometry (EDS). *Mater Struct* 48(7):2043–2062
39. Lim S, Akiyama M, Frangopol DM, Jiang H (2017) Experimental investigation of the spatial variability of the steel weight loss and corrosion cracking of reinforced concrete members: novel X-ray and digital image processing techniques. *Struct Infrastruct Eng* 13(1):118–134